Chemical Geology 420 (2016) 180–185

Contents lists available at ScienceDirect

Chemical Geology

journal homepage: www.elsevier.com/locate/chemgeo

The impact of dissolved CO_2 on bubble nucleation in water-poor rhyolite melts

James E. Gardner [a,*], James D. Webster [b]

[a] Department of Geological Sciences, Jackson School of Geosciences, The University of Texas at Austin, Austin, TX 78712-0254, USA
[b] Department of Earth and Planetary Sciences, American Museum of Natural History, Central Park West at 79th, New York, NY 10024-5192, USA

ARTICLE INFO

Article history:
Received 3 August 2015
Received in revised form 13 November 2015
Accepted 16 November 2015
Available online 1 December 2015

Keywords:
Bubble
Nucleation
Rhyolite
Kinetics
H_2O
CO_2

ABSTRACT

Volcanic eruptions of H_2O-poor rhyolite are enigmas, because gas bubbles are needed to drive eruptions, but experimental evidence suggests that bubbles cannot nucleate because there is insufficient H_2O to overcome the free energy associated with the formation of the bubble–melt interface. In this study, we examine whether CO_2 in the melt can solve that enigma, possibly by nucleating CO_2-enriched bubbles that are then used by H_2O or lowering the surficial free energy. We use experimental decompressions to examine the affect of dissolved CO_2 at conditions both where H_2O alone can nucleate bubbles, and where H_2O activity is too poor to nucleate bubbles. Experiments using CO_2-free, hydrated rhyolite melt at 875–900 °C conditions find that bubbles nucleate when $[H_2O] = 4.34$–4.74 wt.%, once H_2O supersaturates (Δc, the ratio of the initial H_2O content to the expected amount at equilibrium at low pressure) by ~2–3. Rhyolite melts with less H_2O do not nucleate bubbles, even when $\Delta c \gg 3$. Equally hydrated rhyolite melt that also contains 500–1000 ppm CO_2 nucleates bubbles similarly in terms of the critical Δc, except that CO_2-bearing rhyolite must decompress more to reach a given Δc. That difference is just a result of the change in H_2O solubility in the presence CO_2. It thus appears that bubble nucleation in rhyolite melt is dictated by Δc, and does not change in the presence of CO_2. Importantly, molten rhyolite that is too H_2O poor to nucleate bubbles will not nucleate them if they are CO_2 rich. The vesiculation of such melts requires that bubbles nucleate heterogeneously.

1. Introduction

Volcanic eruptions are driven by gas (primarily H_2O) exsolving and growing bubbles in magma as it rises to the surface (Sparks, 1978). While that rise leads magma to become supersaturated in H_2O – where supersaturation (ΔP) is saturation pressure (P_{SAT}) minus low pressure (P) – bubbles will not form until ΔP overcomes the surficial free energy (σ) of the bubble–melt interface (Hurwitz and Navon, 1994; Gonnermann and Gardner, 2013). High values of ΔP are typically needed to homogeneously nucleate H_2O bubbles in rhyolite melt (Mourtada-Bonnefoi and Laporte, 1999, 2002; Mangan and Sisson, 2000; Gardner and Ketcham, 2011). In fact, Mourtada-Bonnefoi and Laporte (1999) found that rhyolite with ~4 wt.% H_2O does not nucleate bubbles, even at $\Delta P \approx P_{SAT}$. Heterogeneities, such as crystals, can reduce ΔP by reducing the effective σ (Hurwitz and Navon, 1994; Mangan et al., 2004; Gardner and Denis, 2004). In their absence, however, bubbles are unlikely to nucleate in H_2O-poor rhyolite melt.

It would thus seem that H_2O-poor rhyolite melts need to be crystal-rich in order to erupt. But aphyric rhyolite that originally had ≤2.5 wt.% H_2O has, for example, erupted both explosively and as obsidian lava at Yellowstone (Fig. 1). How do bubbles nucleate in such H_2O-poor magmas? The Yellowstone rhyolitic magmas are rich in dissolved CO_2 (Fig. 1). That CO_2 could have facilitated degassing, for example, by forming CO_2-dominated bubbles rather than H_2O-rich bubbles, because of the much lower solubility of CO_2 in rhyolite melt (Blank et al., 1993). In that case, H_2O could then degas into those bubbles or the CO_2 bubbles could serve as sites for heterogeneous H_2O bubble nucleation. At present, evidence for the effects of CO_2 in H_2O-poor rhyolite melts is sparse. Mangan and Sisson (2000) suggest that CO_2 has no affect on homogeneous bubble nucleation. But, only one of their samples that was decompressed fast enough (8.5 MPa s^{-1}) to induce homogeneous nucleation contained more than 20 ppm CO_2, and it was decompressed only to moderate ΔP. Bai et al. (2008) suggest that significant amounts of CO_2 can affect bubble nucleation in hydrous basalt, but the conditions of their experiments were such that bubbles could nucleate without CO_2 present, and so it is unclear whether CO_2 allows degassing when H_2O alone cannot. In a more extensive study, Mourtada-Bonnefoi and Laporte (1999, 2002) found that rhyolites with ~4.5 wt.% H_2O and significant CO_2 (≥800 ppm) nucleated bubbles upon decompression, whereas similar melts with little CO_2 did not.

This study builds on the work of Mourtada-Bonnefoi and Laporte (1999, 2002), by comparing bubble nucleation in hydrous rhyolite melt that either does or does not contain CO_2. We examine conditions

* Corresponding author.
E-mail address: gardner@mail.utexas.edu (J.E. Gardner).

http://dx.doi.org/10.1016/j.chemgeo.2015.11.017
0009-2541/

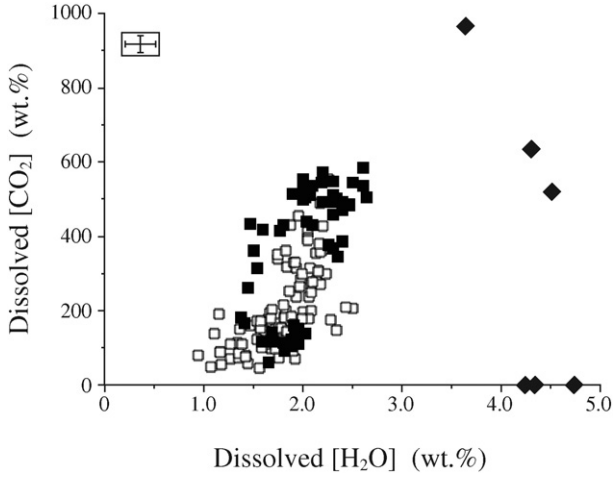

Fig. 1. Dissolved H_2O and CO_2 contents of rhyolitic glass inclusions in quartz phenocrysts from 6 obsidian lavas (open squares) and 3 pyroclastic tuffs (filled squares), erupted in the past 175 k.y. at Yellowstone caldera (K. Befus and J.E. Gardner, unpublished data). The average errors ($\pm 1\sigma$) on analyses are shown. Volatile contents of rhyolite glasses used in this study are shown as diamonds, with error bars smaller than the symbol size (Table 2).

both at which H_2O can nucleate bubbles, and at which H_2O is poor to nucleate bubbles, in order to examine whether CO_2 facilitates bubble nucleation.

2. Material and methods

All experiments used cylinders cored from obsidian that has been used by this lab before (Gardner, 2009; Gardner and Ketcham, 2011; Gardner et al., 2013). It consists of high-silica rhyolitic glass and <1 vol.% microlites of Fe–Ti oxides (Table 1). Most cylinders were 11–13 mm long and 2.7 mm in diameter.

Six cylinders and sufficient distilled water were sealed inside Au capsules, and each capsule was placed into externally heated, cold-seal pressure vessels and run at 875° or 900 °C (±5 °C) and 120, 125, or 140 MPa (±0.1 MPa) for 5–6 days (Table 2). Six other cylinders were saturated with $H_2O + CO_2$ in an internally heated pressure vessel (IHPV). Two of those were first hydrated at 65 MPa for 5 days, and then re-equilibrated together with a mixed $H_2O + CO_2$ fluid inside a single Pt capsule at 270 MPa and 1000 °C, producing glasses with 3.64 wt.% H_2O and 966 ppm CO_2 (Table 2). Both oxalic acid dihydrate and silver oxalate were used as CO_2 sources. Two other cylinders were hydrated at 135 MPa, and then re-equilibrated with a mixed $H_2O + CO_2$ fluid (oxalic acid dihydrate) in one capsule at 260 MPa and 1000 °C, producing glasses with 4.51 wt.% H_2O and 520 ppm CO_2. The last two cylinders were equilibrated together in a single capsule with a mixed $H_2O + CO_2$ fluid (oxalic acid dihydrate) at 258.5 MPa and 1075 °C, producing glasses with 4.30 wt.% H_2O and 635 ppm CO_2.

Table 1
Rhyolites used in this study and by Mourtada-Bonnefoi and Laporte (1999, 2002).

	This Study	*M-B&L*
SiO_2	76.53	76.51
TiO2	0.06	0.03
Al_2O_3	13.01	12.56
FeO*	0.79	0.55
MnO	0.08	0.07
MgO	0.02	0.01
CaO	0.74	0.25
Na_2O	3.87	4.47
K_2O	4.91	4.24
Molar N/NK	0.55	0.62
Molar A/CNK	0.99	1.01

Composition of sample used in this study measured by electron microprobe (normalized to 100%), with all Fe reported as FeO; oxides are in wt.%.

Samples were extracted from their capsules, and sectioned into smaller samples using a slow speed saw. Each was ~0.5 cm long and weighed ≥50 mg. A thin wafer (~1 mm thick) was also sliced from the center of each sample and used to measure volatile contents using Fourier-Transform Infrared (FTIR) Spectroscopy (see below). More than one wafer was cut from each of the $H_2O + CO_2$ samples to assure that volatiles were homogeneously distributed in the glasses.

Each sample cut from the starting materials was used in a decompression experiment by sealing it inside Au capsules, which were then placed into a cup on the end of an Inconel rod and inserted into rapid-quench, cold-seal pressure vessels. The sample was held in the water-cooled region of the vessel while the pressure vessel heated to 850 or 875 °C. The Inconel rod was then raised with an external magnet to insert the sample into the hot zone of the pressure vessel. Pressure was quickly adjusted using a hand-operated intensifier to either 1 MPa above the original hydration pressure or to 251 MPa (Table 2). Although that latter pressure differs slightly from the original pressures, the difference did not induce bubbles to nucleate, as shown by the absence of bubbles after most decompressions.

After a sample heated for 5 min, pressure was released quickly to a lower pressure (P_{FINAL}), and then held there for a given amount of time before the sample was rapidly quenched by lowering it back into the water-cooled jacket. The method of pressure release changed during the project. At first, the pressure line was cracked open to release water from it until pressure had dropped to the desired level. These were relatively slow (5–22 s) and precise to ±1 s. All of these runs were quenched after a total of 60 s (Table 2). After some trial and error, we changed to dropping pressure by opening the pressure vessel to a large pressure reservoir that had been set at some low pressure. This caused very rapid drops in pressure (≤2.5 s) that could be timed more precisely (±0.1 s). All of these runs were held at P_{FINAL} for ~60 s, except one which was held for ~120 s. Except for that one, the amount of time that all samples spent below the starting pressure was ~60 s (Table 2).

All decompression samples were examined to see whether bubbles nucleated (Fig. 2). If they had, their number density (N_B) was measured using a petrographic microscope by selecting 4–5 areas (40 μm × 40 μm) of a sample and counting all bubbles that appear as the field of view is moved through it using the focusing knob of the microscope. The thickness of each volume measured, typically 800–2000 μm, was recorded by a Heidenhain focus drive linear encoder that detects the motion of the stage, and is precise to ±0.6 μm. The typical volume was ~9.6×10^{-3} cm^{-3}, and so the detection limit on N_B is ~100 cm^{-3}.

Dissolved volatiles were analyzed with a Thermo Electron Nicolet 6700 spectrometer and Continuμm IR microscope. Concentrations of molecular (H_2O_m) and hydroxl (OH^-) H_2O in glasses were determined from absorbances at ~5250 and ~4500 cm^{-1}, using white light and a CaF_2 beamsplitter and the model of Zhang et al. (1997). Reported H_2O contents are the averaged sums of H_2O_m and OH^- (Table 2). The same spots were analyzed for dissolved molecular CO_2, which was determined from the absorbance at ~2350 cm^{-1}, using a globular light source and a KBr beamsplitter and the absorptivity of Behrens et al. (2004). Sample thicknesses were measured with the focus drive encoder described above.

3. Results

Numerous bubbles (often <10 μm) grew in the outer fringes of all decompression samples (Fig. 2a). Such "fringe" bubbles occur almost invariably in decompressions of hydrous melts, and result from heterogeneous nucleation where the melt touches the metal capsule (Mangan and Sisson, 2000). In this study we ignore these bubbles, and instead focus on the interiors of samples, away from all contacts, as we are interested in the ability of water-poor rhyolite to nucleate bubbles homogeneously.